Superconductor-altermagnet memory functionality without stray fields

Hans Gløckner Giil ● and Jacob Linder

Center for Quantum Spintronics, Department of Physics, Norwegian University of Science and Technology, NO-7491 Trondheim, Norway

A novel class of antiferromagnets, dubbed altermagnets, exhibit a nonrelativistically spin-split band structure reminiscent of the order parameter phase d-wave superconductors, despite the absence of net magnetization. This unique characteristic enables utilization in cryogenic stray-field-free memory devices, offering the possibility of achieving high storage densities. We here determine how a proximate altermagnet influences the critical temperature T_c of a conventional s-wave singlet superconductor. Considering both a bilayer and trilayer, we show that such hybrid structures may serve as stray-field-free memory devices where the critical temperature is controlled by rotating the Néel vector of one altermagnet, providing infinite magnetoresistance. Furthermore, our study reveals that altermagnetism can coexist with superconductivity up to a critical strength of the altermagnetic order as well as robustness of the altermagnetic influence on the conduction electrons against nonmagnetic impurities, ensuring the persistence of the proximity effect under realistic experimental conditions.

I. INTRODUCTION

The intricate interplay of superconductivity and magnetism remains a focal point in modern condensed matter physics [1–3]. Its allure stems both from a fundamental viewpoint and cryogenic technology applications such as extremely sensitive detectors of radiation and heat as well as circuit components such as qubits and dissipationless diodes. Whereas superconductor-ferromagnet (SC-FM) structures have been studied extensively, the interest in antiferromagnetic materials has been comparatively limited [4–9] up until recently [10–22].

A particularly interesting new development is antiferromagnets that break time-reversal symmetry and feature a spin-split band structure that does not originate from relativistic effects such as spin-orbit coupling. Dubbed altermagnets in the literature, these are spin-compensated magnetic systems with a huge momentum-dependent spin splitting even in collinearly ordered antiferromagnets. *Ab initio* calculations have identified several possible material candidates that can host an altermagnetic state, including metals such as RuO_2 and Mn_5Si_3 as well as semiconductors/insulators such as MnF_2 and La_2CuO_4 [23–28].

Superconducting memory devices with infinite magnetoresistance have been proposed [29,30] and observed [31] using superconducting spin valves, a trilayer configuration comprised of a central superconductor flanked by two ferromagnets. By exploiting the inverse proximity effect, the critical temperature T_c of the superconductor can be dynamically modulated through manipulation of the relative magnetization orientations. In this way, T_c changes up to 1 K have been reported [32]. However, the property enabling the functionality of such structure via external fields is also its drawback, depending on the precise mode of operation: the magnetization. The disadvantage is the inevitable existence of a stray field surrounding the structure, which limits how closely multiple structures of this type can be packed

together without disturbing each other. Therefore, finding a way to control T_c in a structure without any net magnetization could offer a major advantage to the implementation of such architecture in cryogenic devices. Recent strides in unraveling the altermagnet/superconductivity interplay encompass a spectrum of phenomena, including studies of Andreev reflection [33,34], Majorana zero modes [35], the Josephson effect [36–38], and interplay with spin-orbit interaction [39].

We here determine the effect of the altermagnetic spin splitting on the critical temperature of an adjacent superconductor and suggest using an AM-SC-AM trilayer as a stray-field-free memory device. Commencing our study, we investigate a simple model demonstrating coexistence of altermagnetism and superconductivity and show that the altermagnetic field is detrimental to the superconducting order parameter, akin to the Pauli limit in superconductors subjected to magnetic fields [40]. Progressing to AM-SC bilayers, we unveil a modulation in the critical temperature, caused by the altermagnetic order. This modulation is nonmonotonic as a function of the altermagnetic strength, and can both suppress or increase T_c compared to the normal metal case. We explore different geometries, showing that the relative direction of the interface and the altermagnetic order parameter yield vastly different results. A study of AM-SC-AM trilayers is then performed, highlighting the influence of the parallel or antiparallel directions of the order parameters in the two altermagnets. Finally, we investigate the role of impurities in the altermagnetic material. We find that impurities do not suppress the influence of altermagnetic spin order on the itinerant electrons, making the altermagnetic proximity effect relevant even in experiments utilizing materials that have a short mean-free path.

II. THEORY

The lattice Bogoliubov-de Gennes (BdG) framework [41,42] is suitable for studying AM-SC heterostructures.

We employ an attractive Hubbard Hamiltonian to model a conventional phonon-mediated s-wave singlet superconductor:

$$H_{\mathrm{U}} = -\sum_i U_i c_{i\downarrow}^\dagger c_{i\uparrow}^\dagger c_{i\uparrow} c_{i\downarrow}, \tag{1}$$

where $c_{i\sigma}$ and $c_{i\sigma}^\dagger$ destroy and create an electron with spin σ, and $U_i > 0$ is the magnitude of the attractive potential. The attractive Hubbard U term generally differs from the effective electron-electron interaction mediated by phonons (obtained by performing a Schrieffer-Wolff transformation) in terms of momentum and spin indices. Nevertheless, at the mean-field level these models give the same result for the conventional BCS channel for Cooper pairing. We define $b_i = c_{i\downarrow} c_{i\uparrow}$ and perform a mean-field expansion $b_i = \delta b_i + \langle b_i \rangle$, ignoring second-order terms in the deviation from expectation values. Finally, we define a (site-dependent) superconducting order parameter

$$\Delta_i = U_i \langle c_{i\uparrow} c_{i\downarrow} \rangle, \tag{2}$$

and arrive at the mean-field Hamiltonian

$$H_{\mathrm{mf}} = -\sum_i (\Delta_i c_{i\downarrow}^\dagger c_{i\uparrow}^\dagger + \Delta_i^* c_{i\uparrow} c_{i\downarrow}), \tag{3}$$

where we disregarded a constant term, which is absorbed in the ground-state energy.

We note that a constant on-site potential $U_i = U$ corresponds to an isotropic gap in momentum-space that pairs electrons with opposite spin and momentum, which is consistent with the Bardeen-Cooper-Schrieffer theory for an s-wave superconductor. We employ this mean-field superconducting Hamiltonian, including also the effect of altermagnetism and impurities,

$$
\begin{aligned}
H = E_0 &- \sum_{i\sigma} (\mu - w_i) c_{i\sigma}^\dagger c_{i\sigma} - \sum_i (\Delta_i c_{i\downarrow}^\dagger c_{i\uparrow}^\dagger + \Delta_i^* c_{i\uparrow} c_{i\downarrow}) \\
&- \sum_{\langle i,j \rangle \sigma} t_{ij} c_{i\sigma}^\dagger c_{j\sigma} - \sum_{\langle i,j \rangle \sigma\sigma'} (\boldsymbol{m}_{ij} \cdot \boldsymbol{\sigma})_{\sigma\sigma'} c_{i\sigma}^\dagger c_{j\sigma'},
\end{aligned} \tag{4}
$$

where μ is the chemical potential, $\boldsymbol{\sigma} = (\sigma_1, \sigma_2, \sigma_3)$ is the Pauli vector, and w_i is an impurity potential taken to be randomly distributed at a given number of sites in the magnet. For comparison, we consider two different forms of the spin-dependent interaction $\boldsymbol{m}_{ij}$: (i) an on-site potential $\boldsymbol{m}_{ij} = m_z \delta_{ij} \hat{z}$, corresponding to a ferromagnetic term, and (ii) $\boldsymbol{m}_{ij} = +m\boldsymbol{e}_z$ for nearest-neighbor hopping along the x axis and $\boldsymbol{m}_{ij} = -m\boldsymbol{e}_z$ for hopping along the y axis, corresponding to an effective altermagnetic term, similar to what was used in Ref. [36]. The spin-dependent hopping term parametrized by $\boldsymbol{m}_{ij}$ in our Hamilton operator can be understood as a Coulomb-exchange interaction experienced by electrons that are hopping on top of a background of localized spins that form collinear antiferromagnetic order [27]. For a bulk altermagnet, the spin-dependent hopping used in this paper as well as in Ref. [36] takes exactly the cosine form suggested discussed in Refs. [27,43,44], when Fourier transforming to momentum space. Moreover, both the Hubbard model [45,46] and the tight-binding model with spin coupling between itinerant and localized spins have recently been used [47] to derive dispersions that qualitatively match the low-energy form of

the cosine Hamiltonian. The effect of the antiferromagnetic order in the localized spins exerted on the itinerant fermions $\{c_{i\sigma}, c_{i\sigma}^\dagger\}$ in the Hamiltonian Eq. (4) is thus modeled via $\boldsymbol{m}_{ij}$, owing to the fact that this is an effective model for the conduction electrons which breaks the PT-symmetry required to have a spin-split altermagnetic band structure. Formally, one could in principle solve self-consistently for the parameter m in the altermagnet to determine how it is affected by superconductivity. This would be relevant for spontaneous and intrinsic coexistence of altermagnetism and superconductivity in the same material. Instead, we take m to be a fixed constant and solve for Δ self-consistently. This scenario is experimentally relevant in a scenario where the altermagnetic spin splitting has been induced by placing a thin superconductor on top of an altermagnet, stacking them along the z direction, whereas the spin splitting of the bands is present in the k_x-k_y plane. This is similar to what has been done experimentally in thin ferromagnetic insulator/superconductor systems [31,48,49], and obviates the need to solve self-consistently for the spin-splitting parameter as it is induced from an external source. Note that in such a case, the induced m in the superconductor can be smaller than Δ despite the altermagnetic spin splitting in the host material being much larger than Δ. This is because the induced spin splitting via the proximity effect scales with the tunnel coupling to the material, which strongly suppresses its magnitude.

We assume nearest-neighbor hopping, i.e., $t_{ij} = t$, and scale all other parameters in units of t. The superconducting order parameter is determined from the site-dependent self-consistent gap equation in Eq. (2). We assume here that the attraction only occurs in the singlet channel. The singlet phase is more robust than the triplet channel when impurity scattering, which is always present to some extent in real materials, is included. We note that even if the pairing potential only exists in the singlet channel, triplet superconducting correlations can still be induced via the proximity effect when such a superconductor is in contact with an altermagnet. For a discussion concerning the pairing potential in the triplet channel when superconductivity coexists with altermagnetism, see Ref. [50]. Throughout the paper, we fix $\mu = -t/2$ and $U_i = 1.7t$. The magnetic terms, superconducting order parameters, and impurity potentials are only nonzero in their respective regions. Specifically, the altermagnetic term $\boldsymbol{m}_{ij}$ is finite only when both sites i, j inside are in the altermagnet. Expectation values of physical observables are formally computed by performing a trace (using a complete basis set) over the density matrix ρ and the matrix representation of the observable under consideration. The details of this density matrix are not needed for the results presented in our work. This is because the superconducting order parameter and other expectation values can in practice be obtained self-consistently without explicitly computing ρ first, the reason being that expectation values of creation-annihilation pairs of the diagonalized quasiparticle operators give Fermi-Dirac distribution functions.

III. METHODOLOGY

At each site i, the fermionic operators can be organized into Nambu vectors $\hat{c}_i \equiv (c_{i\uparrow}, c_{i\downarrow}, c_{i\uparrow}^\dagger, c_{i\downarrow}^\dagger)$, which may in turn be collected into a $4N$-element vector $\check{c} \equiv (\hat{c}_1, \ldots, \hat{c}_N)$

encompassing all fermionic lattice operators. The Hamiltonian operator is subsequently represented using a $4N \times 4N$ matrix: $H = E_0 + \frac{1}{2}\check{c}^\dagger \check{H}\check{c}$. We solve the BdG equation by numerically diagonalizing $\check{H}$ and expressing physical observables such as the superconducting gap in Eq. (2) in terms of its eigenvectors and eigenvalues. This process entails an initial guess Δ_g for the order parameter, and then self-consistently diagonalizing the Hamiltonian until the superconducting gap equation converges. In this paper, however, our main interest is the critical temperature T_c, and thus we do not need the explicit numerical value of the gap. With that said, we typically find a low-temperature gap magnitude of order $\Delta \simeq 0.15t$ with our parameters. Instead, we perform N_Δ self-consistent iterations and compare the resulting value of the order parameter with the small initial value $\Delta_g = 10^{-4}t$. This solution strategy is very similar to the methodology used, e.g., in Ref. [51]. We define the SC as being in the superconducting state when the median value of the order parameter inside the superconductor has increased compared to the initial value Δ_g. The critical temperature is subsequently ascertained by performing a binomial search in critical temperatures, as was done in Ref. [52]. In order to make the computational time manageable, it is necessary to consider a lattice size that is much smaller than in an experimental setting. For instance, in order to ensure that the width of the superconducting layer is comparable to the superconducting coherence length, which is inversely proportional to Δ, one must use a large value for the superconducting order parameter. Nevertheless, the BdG lattice framework is known to give predictions that compare well, both qualitatively and quantitatively, with experimentally realistic systems [53,54] as long as the ratio of the length scales in the problem (such as the width of the system and the coherence length) is reasonable, which is the approach we have taken.

IV. RESULTS AND DISCUSSION

A. Altermagnetic destruction of the superconducting order

Prior to delving into heterostructures of superconductors and altermagnets, it is instructive first to understand the effects of the altermagnetic term in Eq. (4) on the superconducting order, and employ periodic boundary conditions along both axes. To this end, we consider a system with coexisting altermagnetic and superconducting order. We vary the altermagnetic strength m and calculate the critical temperature self-consistently using the methodology outlined above. The results are shown in Fig. 1: the effect of altermagnetism is to suppress the superconducting order, which vanishes for an altermagnetic strength of $m \approx 0.05t$. The results are juxtaposed with the effects of ferromagnetism, which also suppresses the superconductivity in a similar way, as is well known [40,55], although the critical field is much larger than in the altermagnetic case. We note that in general there exists additional solutions to the self-consistency equation besides the one shown in the top pane of Fig. 1, such as $\Delta = 0$. These solutions have a higher free energy than the solution for Δ that we have presented. Thus, we are presenting the solution for Δ, which corresponds to the thermodynamic ground state of the system. These unstable branches are discussed in detail in the Appendix of Ref. [56].
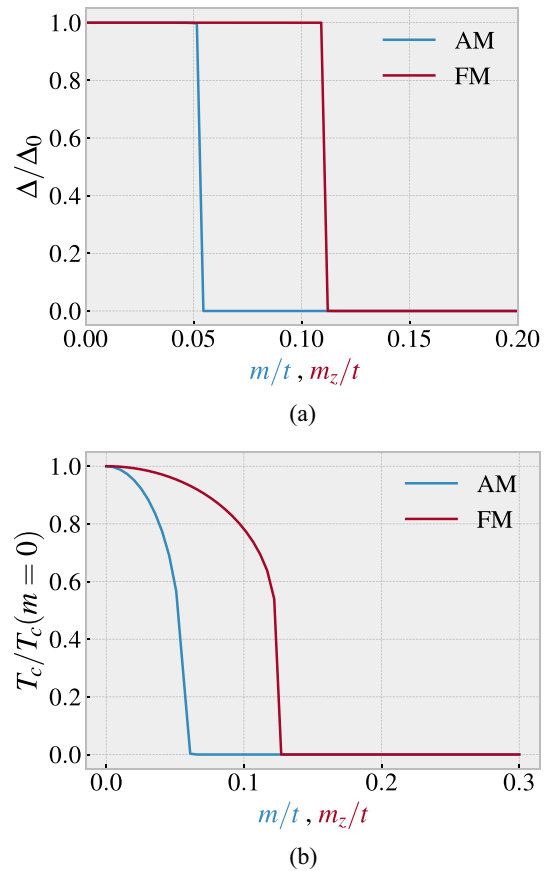

FIG. 1. The (a) order parameter and (b) critical temperature as a function of the altermagnetic and ferromagnetic strength in a $N_x = N_y = 20a_0$ structure with coexisting superconductivity and altermagnetic/ferromagnetic spin splitting. The termperature in (a) is set to $T = 0.01t/k_B$, where k_B is the Boltzmann constant.

After establishing the analogous interaction between the altermagnetic and ferromagnetic terms with superconductivity, a natural inquiry arises regarding the impact of altermagnets on superconductors within heterostructures. Specifically, we will focus our attention on the influence of altermagnets on the critical temperature within AM-SC systems.

B. Junction geometries

Employing a square lattice with lattice constant a_0, we explore two distinct AM-SC geometries: a straight junction, where the interface is aligned with the crystallographic axis, and a skewed junction, where the interface is rotated 45° compared with the crystallographic axis, see Fig. 2. Here, and in the rest of the paper, we employ periodic boundary conditions along the axis parallel to the interface, and hard wall boundary conditions along the axis perpendicular to the interface. We denote the number of lattice sites in the x (y) direction by $N_{x(y)}$. In the straight junction, hopping across the interface happens exclusively along the x axis, while in the skewed junction, hopping across the interface happens equally along the x and y axis. The inverse proximity effect in the SC-AM system can be probed by calculating the critical temperature T_c in the SC. The result is depicted in Fig. 2, highlighting a significant disparity in the behavior between the straight and skewed

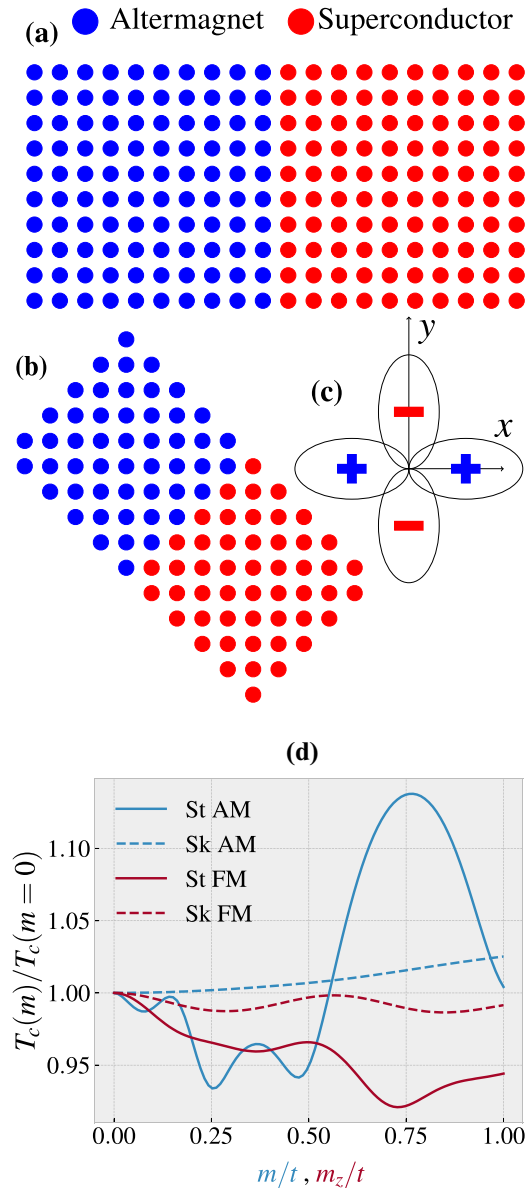**(a)** ... **(b)** ... **(c)** ... **(d)**

FIG. 2. (a) The straight junction and (b) the skewed junction geometries. (c) The hopping term for a spin-up (spin-down) electron (hole). For a spin-down (spin-up) electron (hole), the signs are reversed. (d) The critical temperature for the straight (St) and skewed (Sk) geometries with $N_y = 20a_0$, $N_x^{AM} = 10a_0$, $N_x^{SC} = 6a_0$, and $N_\Delta = 50$.

junction configurations. We emphasize that the normalization in this figure is the critical temperature in a superconductor in contact with a $m = 0$ altermagnet, i.e., a normal metal. Hence, the critical temperature is never raised compared to the critical temperature in the bulk superconductor, but it is raised compared to the critical temperature in a superconductor in proximity with a normal metal. In the skewed junction, the effect of the altermagnetism is to suppress Andreev reflection [57], which is the underlying mechanism causing the (inverse) proximity effect. This happens because the altermagnetic term causes different hopping for electrons and holes involved in Andreev reflection. Thus, the inverse proximity effect is suppressed for high values of m, causing the
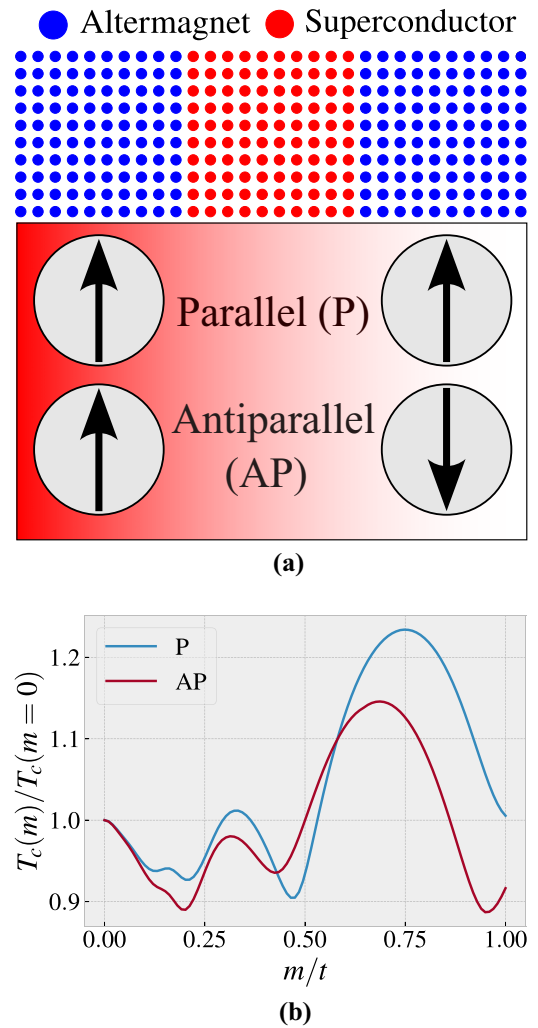

(a)

(b)

FIG. 3. (a) The AM-SC-AM system with P and AP alignment of the altermagnets. (b) The critical temperatures in a system where the length of the SC is $12a_0$, and $N_y = 20a_0$. The altermagnets on either side have a length of $10a_0$.

critical temperature to increase. In the case of the straight junction, an additional factor comes into play—induced magnetization brought about by the inverse proximity effect [58]. This phenomenon leads to a pronounced oscillatory behavior in the critical temperature. The induced magnetization can be understood by noting that spin-up electrons favor hopping in the x direction, causing leaking spin-up electrons from the SC into the AM to be trapped in the AM for large m. In the skewed junction, this effect is averaged out, and the induced magnetization in the SC vanishes.

C. AM-SC-AM trilayers

An intriguing extension to the discussion above can be achieved by adding another altermagnet to the AM-SC system considered above. This system entails two distinct scenarios: one where the two altermagnets are aligned and one where the second altermagnet is rotated (in real space) by 90°. We refer to these situations as a parallel (P) and antiparallel (AP) alignment, see Fig. 3. Rotating the second altermagnet is akin

(a)

(b)

(c)

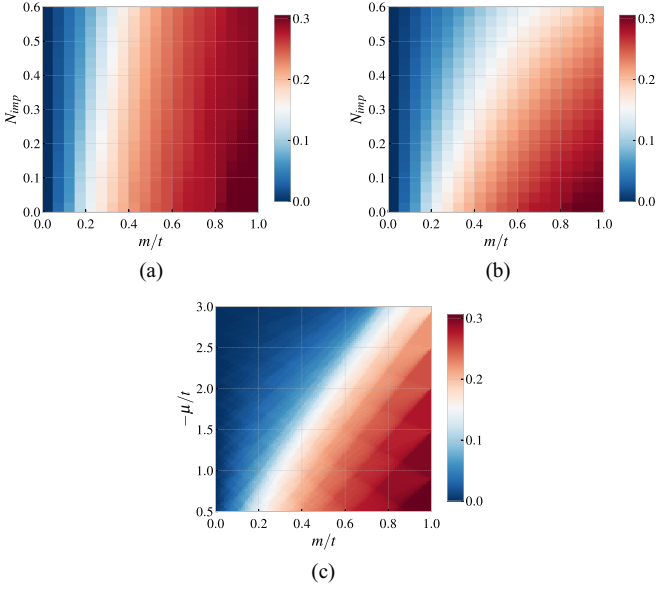FIG. 4. $\Delta C_\uparrow$ as a function of m and N_i, for impurity strength of (a) $w_i = 1t$ and (b) $w = 3t$. (c) $\Delta C_\uparrow$ as a function of m and μ in a system without impurities., The system size is $N_x = N_y = 20a_0$.

to changing the sign of m in this region, or equivalently to a 180° rotation in spin space. In Fig. 3(b), the critical temperature of the SC is calculated for different values of m in the two different systems. In the P alignment, the situation is analogous to the AM-SC system considered above, and we see a similar T_c modulation pattern. In the AP alignment case, the critical temperature is lower than in the P alignment for most values of m. To understand why this is the case, we note that the superconducting coherence length in our system $\xi_S = \hbar v_F / \pi \Delta_0$, where $v_F = \langle |dE_k/d\boldsymbol{k}| \rangle / \hbar$ is the normal state Fermi velocity, where $\langle \ldots \rangle$ represents averaging over the Fermi surface, which can be calculated by introducing periodic boundary conditions along both axes [51], is comparable to the system length. This is typically the regime investigated experimentally. In light of this, we attribute the lower critical temperature to the appearance of crossed Andreev reflection (CAR), sometimes referred to as nonlocal Andreev reflection [59]. It is well known that for an F-S-F heterostructure, the AP alignment of ferromagnets gives enhanced CAR compared to the P alignment [60], and we attribute the results of Fig. 3(b) to a similar origin. The CAR process (strictly speaking, inverse CAR) breaks up a Cooper pair into electrons that become spatially separated in different leads, thus suppressing the superconducting condensate. As more Cooper pairs are transmitted out of the SC due to CAR, the critical temperature drops accordingly. Importantly, switching between the P and AP alignment can experimentally be performed by rotating the Néel vector, since this effectively switches the spin-up and spin-down bands in the altermagnet. A similar T_c modulation in conventional antiferromagnets was very recently reported [61]. Notably, the Néel vector has been found to be controllable by spin-transfer torques [62,63], spin-orbit torques [64], and by optical methods [65]. This opens the possibility of using the suggested device as a stray-field-free memory device operating in the THz regime, enabling the prospect of ultrafast switching.
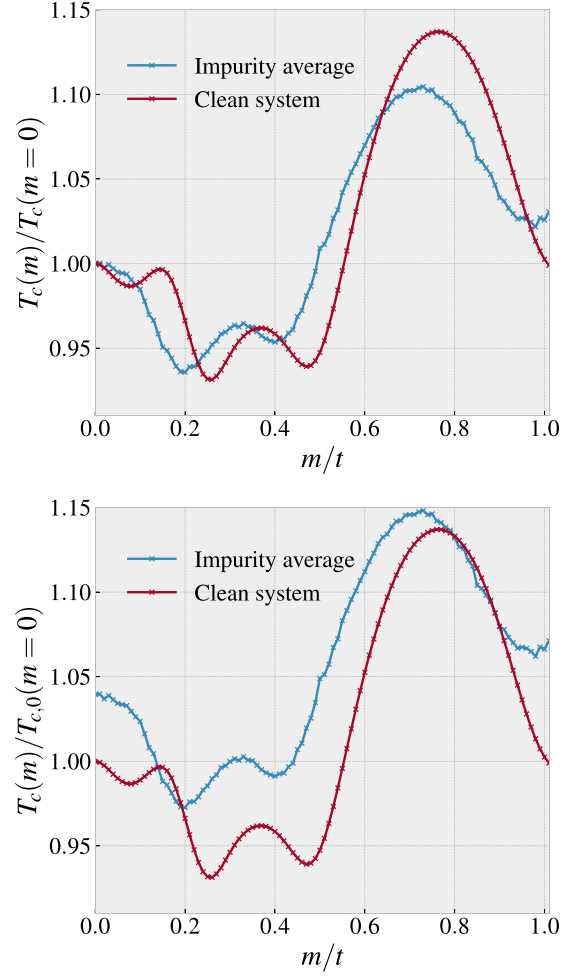

FIG. 5. The impurity average plotted together with the clean system, which is the same as the straight system in Fig. 2(b). In the bottom pane, the temperatures are normalized to the zero-impurity and zero-magnetism critical temperature $T_{c,0}(m = 0)$, showing that T_c is slightly higher in the presence of impurities. In the top pane, the temperatures are normalized to unity for $m = 0$, i.e., the two curves are normalized by a different factor, which illustrates that the variation in T_c with m is of similar magnitude in both cases.

D. Impurity scattering

Materials with substantial impurity scattering are highly relevant for experiments. For this reason, we will concentrate on the role of impurities in altermagnets, before moving on to the proximity effect in a system with a dirty altermagnet. Impurities are accounted for through an on-site potential [66–68] at a fraction N_i of all sites, with a fixed strength w_i, and randomly chosen sites in the altermagnet, similar to the methodology in Ref. [68]. Observables are calculated by averaging over 100 different impurity configurations. As the impurity scattering is isotropic, one might expect that the altermagnetic spin splitting, which is anisotropic, disappears in the presence of impurities. To test this, we define the *bona fide* order parameter $\Delta C_\uparrow$,

$$\Delta C_\uparrow = \sum_i [\langle c_{i\uparrow}^\dagger c_{i+\hat{x}\uparrow} \rangle - \langle c_{i\uparrow}^\dagger c_{i+\hat{y}\uparrow} \rangle], \tag{5}$$

which is a measure of the anisotropy of the effective hopping parameter (for spin-up particles) in the system, and depends on both t and m in general. For square systems, we expect the system to be invariant under C_4 rotations for $m = 0$, i.e., $\Delta C_\uparrow = 0$. Thus, we can use $\Delta C_\uparrow$ to determine whether the system is alternmagnetic or not. In Fig. 4, we plot the results for different values of m and N_i, for $w_i = 1.0t$ and $w_i = 3.0t$, comparable to other values used in the literature [67]. Evidently, the alternmagnetic order is resilient to the nonmagnetic impurities in the system; the slight suppression of the order parameter for strong impurity scattering [i.e., the upper parts of the plots in Figs. 4(b) and 4(a)] can be explained by the fact that the impurities takes the form of local chemical potentials. Hence, a high concentration of impurities has the effect of an effective renormalized global chemical potential. To show this, we calculate the order parameter $\Delta C_\uparrow$ for different values of global chemical potentials, as shown in Fig. 4(c). The suppression of the order parameter for high absolute values of μ is similar to the behavior of the order parameter for high impurity configurations in Figs. 4(a) and 4(b). The reason for the dependence of the order parameter magnitude on μ is that the latter determines the filling factor and density of states at the Fermi level, which in turn affects the superconducting pairing.

Finally, we repeat the calculations of the straight junction in Fig. 2, including impurities in the AM. We set the strength of the impurities to $w_i = 1.0t$ and the fraction of sites occupied by impurities to 0.2, and perform the calculations for 100 different impurity configurations, before averaging over the resulting values of the critical temperature. The results are shown in Fig. 5, and show that although the critical temperature curve is different from the clean system, the (inverse) proximity effect is still present, which is evident from the fact that the critical temperature varies with a similar magnitude compared with the clean system.

Thus, we conclude that impurities are not strongly detrimental to the alternmagnetic modulation of the superconducting order, which means that the effect should be experimentally visible even for dirty materials. We have thus found that the analogy between d-wave superconductor and alternmagnetism [28] is not useful in impurity considerations: whereas d-wave superconductivity is highly sensitive to nonmagnetic impurities, the alternmagnetic effect on the conduction electrons survives even in the presence strong impurity potentials. This is due to the d-wave Fermi surface of alternmagnets being spin split, prohibiting the scattering between the spin bands in the absence of spin-flip impurities.

V. CONCLUSION

We have solved the lattice Bogoliubov-de Gennes equations in heterostructures of superconductors and alternmagnets. Our study indicates that alternmagnetic materials have the potential to be used in cryogenic spintronic devices, for instance as stray-field-free spin switches showing infinite magnetoresistivity, using spin-transfer torques, spin-orbit torques, or optical methods to rotate the Néel vector. Nonmagnetic impurities are not severely detrimental to the alternmagnetic proximity effect, allowing for this effect to be present also in alternmagnetic materials in the diffusive transport regime.

[1] F. S. Bergeret, A. F. Volkov, and K. B. Efetov, Odd triplet superconductivity and related phenomena in superconductor-ferromagnet structures, Rev. Mod. Phys. **77**, 1321 (2005).

[2] A. I. Buzdin, Proximity effects in superconductor-ferromagnet heterostructures, Rev. Mod. Phys. **77**, 935 (2005).

[3] F. S. Bergeret, M. Silaev, P. Virtanen, and T. T. Heikkilä, Colloquium: Nonequilibrium effects in superconductors with a spin-splitting field, Rev. Mod. Phys. **90**, 041001 (2018).

[4] B. M. Andersen, I. V. Bobkova, P. J. Hirschfeld, and Y. S. Barash, $0 - \pi$ transitions in Josephson junctions with antiferromagnetic interlayers, Phys. Rev. Lett. **96**, 117005 (2006).

[5] B. M. Andersen, I. V. Bobkova, P. J. Hirschfeld, and Y. S. Barash, Bound states at the interface between antiferromagnets and superconductors, Phys. Rev. B **72**, 184510 (2005).

[6] C. Bell, E. J. Tarte, G. Burnell, C. W. Leung, D.-J. Kang, and M. G. Blamire, Proximity and Josephson effects in superconductor/antiferromagnetic Nb / $\gamma - Fe_{50}Mn_{50}$ heterostructures, Phys. Rev. B **68**, 144517 (2003).

[7] M. Hübener, D. Tikhonov, I. A. Garifullin, K. Westerholt, and H. Zabel, The antiferromagnet/superconductor proximity effect in Cr/V/Cr trilayers, J. Phys.: Condens. Matter **14**, 8687 (2002).

[8] B. L. Wu, Y. M. Yang, Z. B. Guo, Y. H. Wu, and J. J. Qiu, Suppression of superconductivity in Nb by IrMn in IrMn/Nb bilayers, Appl. Phys. Lett. **103**, 152602 (2013).

[9] H. Enoksen, J. Linder, and A. Sudbø, Pressure-induced 0-π transitions and supercurrent crossover in antiferromagnetic weak links, Phys. Rev. B **88**, 214512 (2013).

[10] L. G. Johnsen, S. H. Jacobsen, and J. Linder, Magnetic control of superconducting heterostructures using compensated antiferromagnets, Phys. Rev. B **103**, L060505 (2021).

[11] G. A. Bobkov, I. V. Bobkova, A. M. Bobkov, and A. Kamra, Néel proximity effect at antiferromagnet/superconductor interfaces, Phys. Rev. B **106**, 144512 (2022).

[12] D. S. Rabinovich, I. V. Bobkova, and A. M. Bobkov, Anomalous phase shift in a Josephson junction via an antiferromagnetic interlayer, Phys. Rev. Res. **1**, 033095 (2019).

[13] V. Falch and J. Linder, Giant magnetoanisotropy in the Josephson effect and switching of staggered order in antiferromagnets, Phys. Rev. B **106**, 214511 (2022).

[14] M. F. Jakobsen, K. B. Naess, P. Dutta, A. Brataas, and A. Qaiumzadeh, Electrical and thermal transport in antiferromagnet-superconductor junctions, Phys. Rev. B **102**, 140504(R) (2020).

[15] J. L. Lado and M. Sigrist, Two-dimensional topological superconductivity with antiferromagnetic insulators, Phys. Rev. Lett. **121**, 037002 (2018).

[16] E. H. Fyhn, A. Brataas, A. Qaiumzadeh, and J. Linder, Quasiclassical theory for antiferromagnetic metals, Phys. Rev. B **107**, 174503 (2023).

[17] E. H. Fyhn, A. Brataas, A. Qaiumzadeh, and J. Linder, Superconducting proximity effect and long-ranged triplets in dirty metallic antiferromagnets, Phys. Rev. Lett. **131**, 076001 (2023).

[18] G. A. Bobkov, I. V. Bobkova, and A. M. Bobkov, Proximity effect in superconductor/antiferromagnet hybrids: Néel triplets and impurity suppression of superconductivity, Phys. Rev. B **108**, 054510 (2023).

[19] S. Chourasia, L. J. Kamra, I. V. Bobkova, and A. Kamra, Generation of spin-triplet Cooper pairs via a canted antiferromagnet, Phys. Rev. B **108**, 064515 (2023).

[20] E. Erlandsen and A. Sudbø, Schwinger boson study of superconductivity mediated by antiferromagnetic spin fluctuations, Phys. Rev. B **102**, 214502 (2020).

[21] E. Thingstad, E. Erlandsen, and A. Sudbø, Eliashberg study of superconductivity induced by interfacial coupling to antiferromagnets, Phys. Rev. B **104**, 014508 (2021).

[22] K. Mæland, B. Brekke, and A. Sudbø, Many-body effects on superconductivity mediated by double-magnon processes in altermagnets, arXiv:2402.14061 [cond-mat].

[23] S. Hayami, Y. Yanagi, and H. Kusunose, Momentum-dependent spin splitting by collinear antiferromagnetic ordering, J. Phys. Soc. Jpn. **88**, 123702 (2019).

[24] K.-H. Ahn, A. Hariki, K.-W. Lee, and J. Kuneš, Antiferromagnetism in RuO$_2$ as d-wave Pomeranchuk instability, Phys. Rev. B **99**, 184432 (2019).

[25] S. López-Moreno, A. H. Romero, J. Mejía-López, and A. Muñoz, First-principles study of pressure-induced structural phase transitions in MnF$_2$, Phys. Chem. Chem. Phys. **18**, 33250 (2016).

[26] L. Šmejkal, R. González-Hernández, T. Jungwirth, and J. Sinova, Crystal time-reversal symmetry breaking and spontaneous Hall effect in collinear antiferromagnets, Sci. Adv. **6**, eaaz8809 (2020).

[27] H. Reichlová, R. L. Seeger, R. González-Hernández, I. Kounta, R. Schlitz, D. Kriegner, P. Ritzinger, M. Lammel, M. Leiviskä, V. Petříček, P. Doležal, E. Schmoranzerová, A. Baďura, A. Thomas, V. Baltz, L. Michez, J. Sinova, S. T. B. Goennenwein, T. Jungwirth, and L. Šmejkal, Macroscopic time reversal symmetry breaking by staggered spin-momentum interaction, arXiv:2012.15651 [cond-mat].

[28] L. Šmejkal, J. Sinova, and T. Jungwirth, Beyond conventional ferromagnetism and antiferromagnetism: A phase with nonrelativistic spin and crystal rotation symmetry, Phys. Rev. X **12**, 031042 (2022).

[29] A. I. Buzdin, A. V. Vedyayev, and N. V. Ryzhanova, Spin-orientation–dependent superconductivity in F/S/F structures, Europhys. Lett. **48**, 686 (1999).

[30] L. R. Tagirov, Low-field superconducting spin switch based on a superconductor / ferromagnet multilayer, Phys. Rev. Lett. **83**, 2058 (1999).

[31] B. Li, N. Roschewsky, B. A. Assaf, M. Eich, M. Epstein-Martin, D. Heiman, M. Münzenberg, and J. S. Moodera, Superconducting spin switch with infinite magnetoresistance induced

[32] by an internal exchange field, Phys. Rev. Lett. **110**, 097001 (2013).

[32] A. Singh, S. Voltan, K. Lahabi, and J. Aarts, Colossal proximity effect in a superconducting triplet spin valve based on the half-metallic ferromagnet CrO$_2$, Phys. Rev. X **5**, 021019 (2015).

[33] C. Sun, A. Brataas, and J. Linder, Andreev reflection in altermagnets, Phys. Rev. B **108**, 054511 (2023).

[34] M. Papaj, Andreev reflection at the altermagnet-superconductor interface, Phys. Rev. B **108**, L060508 (2023).

[35] S. A. A. Ghorashi, T. L. Hughes, and J. Cano, Altermagnetic routes to Majorana modes in zero net magnetization, arXiv:2306.09413 [cond-mat].

[36] J. A. Ouassou, A. Brataas, and J. Linder, Dc Josephson effect in altermagnets, Phys. Rev. Lett. **131**, 076003 (2023).

[37] S.-B. Zhang, L.-H. Hu, and T. Neupert, Finite-momentum Cooper pairing in proximitized altermagnets, Nat. Commun. **15**, 1801 (2024).

[38] C. W. J. Beenakker and T. Vakhtel, Phase-shifted Andreev levels in an altermagnet Josephson junction, Phys. Rev. B **108**, 075425 (2023).

[39] M. Wei, L. Xiang, F. Xu, L. Zhang, G. Tang, and J. Wang, Gapless superconducting state and mirage gap in altermagnets, arXiv:2308.00248 [cond-mat].

[40] A. M. Clogston, Upper limit for the critical field in hard superconductors, Phys. Rev. Lett. **9**, 266 (1962).

[41] J.-X. Zhu, *Bogoliubov-de Gennes Method and Its Applications*, Lecture Notes in Physics (Springer International Publishing, Cham, 2016), Vol. 924.

[42] P. G. de Gennes, *Superconductivity of Metals and Alloys* (W.A. Benjamin, Boston, 1966).

[43] L. Šmejkal, J. Sinova, and T. Jungwirth, Emerging research landscape of altermagnetism, Phys. Rev. X **12**, 040501 (2022).

[44] L. Šmejkal, A. B. Hellenes, R. González-Hernández, J. Sinova, and T. Jungwirth, Giant and tunneling magnetoresistance in unconventional collinear antiferromagnets with nonrelativistic spin-momentum coupling, Phys. Rev. X **12**, 011028 (2022).

[45] P. Das, V. Leeb, J. Knolle, and M. Knap, Realizing altermagnetism in Fermi-Hubbard models with ultracold atoms, arXiv:2312.10151 [cond-mat.quant-gas].

[46] M. Naka, S. Hayami, H. Kusunose, Y. Yanagi, Y. Motome, and H. Seo, Spin current generation in organic antiferromagnets, Nat. Commun. **10**, 4305 (2019).

[47] B. Brekke, A. Brataas, and A. Sudbø, Two-dimensional altermagnets: Superconductivity in a minimal microscopic model, Phys. Rev. B **108**, 224421 (2023).

[48] S. Kolenda, M. J. Wolf, and D. Beckmann, Observation of thermoelectric currents in high-field superconductor-ferromagnet tunnel junctions, Phys. Rev. Lett. **116**, 097001 (2016).

[49] M. Rouco, S. Chakraborty, F. Aikebaier, V. N. Golovach, E. Strambini, J. S. Moodera, F. Giazotto, T. T. Heikkilä, and F. S. Bergeret, Charge transport through spin-polarized tunnel junction between two spin-split superconductors, Phys. Rev. B **100**, 184501 (2019).

[50] D. Zhu, Z.-Y. Zhuang, Z. Wu, and Z. Yan, Topological superconductivity in two-dimensional altermagnetic metals, Phys. Rev. B **108**, 184505 (2023).

[51] L. G. Johnsen, K. Svalland, and J. Linder, Controlling the superconducting transition by rotation of an inver-

sion symmetry-breaking axis, Phys. Rev. Lett. **125**, 107002 (2020).

[52] J. A. Ouassou, Manipulating superconductivity in magnetic nanostructures in and out of equilibrium, Ph.D. thesis, Norwegian University of Science and Technology, Trondheim, 2019.

[53] A. M. Black-Schaffer and J. Linder, Strongly anharmonic current-phase relation in ballistic graphene Josephson junctions, Phys. Rev. B **82**, 184522 (2010).

[54] C. D. English, D. R. Hamilton, C. Chialvo, I. C. Moraru, N. Mason, and D. J. Van Harlingen, Observation of nonsinusoidal current-phase relation in graphene Josephson junctions, Phys. Rev. B **94**, 115435 (2016).

[55] B. S. Chandrasekhar, A note on the maximum critical field of high- field superconductors, Appl. Phys. Lett. **1**, 7 (1962).

[56] J. A. Ouassou, T. D. Vethaak, and J. Linder, Voltage-induced thin-film superconductivity in high magnetic fields, Phys. Rev. B **98**, 144509 (2018).

[57] A. F. Andreev, The thermal conductivity of the intermediate state in superconductors, Zh. Eksp. Teor. Fiz. **46**, 1823 (1964) [Sov. Phys. JETP **19**, 1228 (1964)].

[58] J. Linder and J. W. A. Robinson, Superconducting spintronics, Nat. Phys. **11**, 307 (2015).

[59] G. Falci, D. Feinberg, and F. W. J. Hekking, Correlated tunneling into a superconductor in a multiprobe hybrid structure, Europhys. Lett. **54**, 255 (2001).

[60] G. Deutscher and D. Feinberg, Coupling superconducting-ferromagnetic point contacts by Andreev reflections, Appl. Phys. Lett. **76**, 487 (2000).

[61] L. J. Kamra, S. Chourasia, G. A. Bobkov, V. M. Gordeeva, I. V. Bobkova, and A. Kamra, Complete T_c suppression and Néel triplets mediated exchange in antiferromagnet-superconductor-antiferromagnet trilayers, Phys. Rev. B **108**, 144506 (2023).

[62] R. Cheng, M. W. Daniels, J.-G. Zhu, and D. Xiao, Ultrafast switching of antiferromagnets via spin-transfer torque, Phys. Rev. B **91**, 064423 (2015).

[63] S. Urazhdin and N. Anthony, Effect of polarized current on the magnetic state of an antiferromagnet, Phys. Rev. Lett. **99**, 046602 (2007).

[64] Z. Xu, J. Ren, Z. Yuan, Y. Xin, X. Zhang, S. Shi, Y. Yang, and Z. Zhu, Field-free spin–orbit torque switching of an antiferromagnet with perpendicular Néel vector, J. Appl. Phys. **133**, 153904 (2023).

[65] V. Grigorev, M. Filianina, Y. Lytvynenko, S. Sobolev, A. R. Pokharel, A. P. Lanz, A. Sapozhnik, A. Kleibert, S. Bodnar, P. Grigorev, Y. Skourski, M. Kläui, H.-J. Elmers, M. Jourdan, and J. Demsar, Optically triggered Néel vector manipulation of a metallic antiferromagnet Mn_2Au under strain, ACS Nano **16**, 20589 (2022).

[66] Y. Asano, Y. Sawa, Y. Tanaka, and A. A. Golubov, Odd-frequency pairs and Josephson current through a strong ferromagnet, Phys. Rev. B **76**, 224525 (2007).

[67] Y. Asano, Y. Tanaka, and A. A. Golubov, Josephson effect due to odd-frequency pairs in diffusive half metals, Phys. Rev. Lett. **98**, 107002 (2007).

[68] Z.-X. Li, S. A. Kivelson, and D.-H. Lee, Superconductor-to-metal transition in overdoped cuprates, npj Quantum Mater. **6**, 36 (2021).